

A Diffusion-Refined Planner with Reinforcement Learning Priors for Confined-Space Parking

Mingyang Jiang, Yueyan Li, Jiaru Zhang, Songan Zhang, and Ming Yang

Abstract—The growing demand for parking has increased the need for automated parking planning methods that can operate reliably in confined spaces. In restricted and complex environments, high-precision maneuvers are required to achieve a high success rate in planning, yet existing approaches often rely on explicit action modeling, which faces challenges when accurately modeling the optimal action distribution. In this paper, we propose DRIP, a diffusion-refined planner anchored in reinforcement learning (RL) prior action distribution, in which an RL-pretrained policy provides prior action distributions to regularize the diffusion training process. During the inference phase the denoising process refines these coarse priors into more precise action distributions. By steering the denoising trajectory through the reinforcement learning prior distribution during training, the diffusion model inherits a well-informed initialization, resulting in more accurate action modeling, a higher planning success rate, and reduced inference steps. We evaluate our approach across parking scenarios with varying degrees of spatial constraints. Experimental results demonstrate that our method significantly improves planning performance in confined-space parking environments while maintaining strong generalization in common scenarios.

Index Terms—Automated parking, diffusion model, reinforcement learning, path planning.

I. INTRODUCTION

The rapid growth of urbanization and vehicle ownership has intensified parking demand and exacerbated space scarcity in modern cities, giving rise to increasingly narrow parking lots and confined environments [1]. Consequently, automated parking has emerged as a critical functionality. A reliable parking path planner can not only reduce accidents and improve efficiency but also accommodate the continuing trend of shrinking parking spaces [2]. Traditional rule-based methods have been widely deployed in relatively simple scenarios [3, 4]. However, their inherent limitations in understanding the surrounding environment often result in planning failures as situations become more complex [5].

To address the limitations of rule-based methods, learning-based approaches, which formulate parking path planning as a sequential action prediction problem, have recently gained prominence for their ability to establish data-driven mappings from environmental observations to driving actions [6]. However, these methods typically rely on explicit action distribution modeling, which has proven inadequate for capturing the intricacies of feasible maneuvers in complex tasks [7]. This is particularly critical in narrow parking scenarios, where high precision is required under non-holonomic constraints. As shown in Fig. 1, even minor inaccuracies in trajectory generation may lead to collisions or excessive corrective

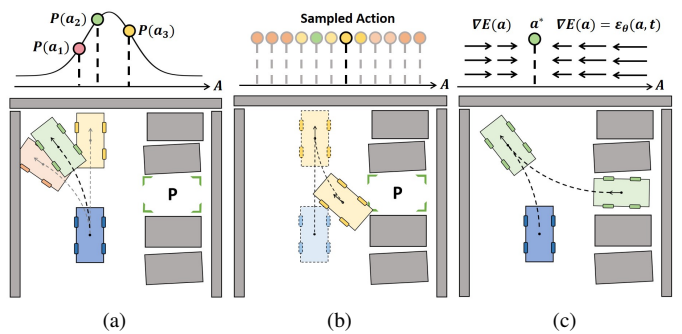


Fig. 1: Comparison between explicit action modeling and diffusion-based policy for parking. (a) An explicit action model parameterizes an action distribution or probabilistic function and selects actions by sampling or maximizing this distribution. This can leave nontrivial mass on suboptimal maneuvers, which in confined spaces leads to collisions or additional corrective steps (b). (c) A diffusion policy models actions implicitly via learning a gradient field and iteratively refines noisy proposals toward feasible, high-precision trajectories.

maneuvers, ultimately reducing the overall success rate of parking [8].

To improve the expressivity of the explicit action modeling policy, recent studies have explored diffusion policies, which formulate the prediction of actions as a conditional denoising diffusion process [7]. By learning to recover structured actions from noisy inputs, diffusion policies offer a flexible generative framework that is well-suited to modeling complex and precise action distributions and tackling the challenges in sequential action prediction.

While diffusion policies were initially developed with imitation learning, reinforcement learning (RL) has demonstrated remarkable effectiveness in sequential action prediction, motivating recent efforts to integrate RL with diffusion to combine the strengths of both paradigms [9]. Existing efforts in this direction mainly adopt an RL training paradigm to fine-tune a diffusion actor [10]. Such methods introduce reward-driven objectives to purely supervised learning-based diffusion policies to achieve better performance. Yet they also encounter challenges, including training instability induced by backpropagation through time (BPTT), difficulties in handling out-of-distribution (OOD) data, and sensitivity to imperfect value estimation [10–12], limit the applicability of existing methods in real applications.

In the task of parking path planning, pretraining a policy with RL is available, suggesting an alternative way to leverage RL beyond fine-tuning. Instead of relying on RL solely as a fine-tuning mechanism, we incorporate an RL-pretrained policy as prior knowledge within the diffusion process. Specifically, the action distribution predicted by the RL-pretrained policy is employed as the start for the denoising initialization, while the denoising process further refines the output distribution into more precise trajectories. To achieve this, we design the training procedure such that denoising trajectories are aligned with the prior action distributions, enabling the model to exploit well-informed initialization during inference and thereby better handle the precision required in confined parking scenarios. Overall, the contributions of this paper are:

- To address the challenge of accurately modeling action distributions in confined parking spaces, we propose **DRIP**, a **D**iffusion-**R**efined **I**nference **P**lanner, which refines reinforcement learning policies and enables RL-pretrained policies to be further optimized for generating precise and feasible maneuvers.
- To align denoising trajectories with prior action distributions, we design a denoising training procedure anchored in the priors, ensuring that inference initialization remains consistent with the diffusion training process.
- We validate our approach in parking scenarios with varying levels of spatial constraints, demonstrating significant performance gains in narrow and confined environments while maintaining strong generalization to diverse common cases.

II. RELATED WORK

A. Parking Path-planning

Parking path planning is particularly challenging due to discontinuous trajectories, non-holonomic constraints, and narrow spaces [13]. Traditional geometric and sampling-based approaches have been widely applied [14, 15], but their limited ability to handle complex environments restricts their effectiveness [16]. With the advancement of deep learning, learning-based approaches have emerged as a promising alternative for parking path planning, directly mapping environmental information to action distributions and thereby addressing some of the limitations of rule-based methods. Existing studies can be broadly divided into imitation learning (IL) and reinforcement learning (RL) paradigms [17].

Imitation learning-based methods include approaches that imitate trajectories optimized by rule-based planners [18], methods that align simulated trajectories with human driving behaviors [19], and behavior cloning approaches that collect input-output data directly from real vehicles [20]. Reinforcement learning-based methods have also been widely investigated. For example, Du et al. trained agents in manually designed simulation environments [21], while Wang et al. reconstructed realistic environments from LiDAR data collected in the real world to support training [22]. Although directly applying standard RL algorithms to the planning problem is feasible for simple cases, studies that combine RL with heuristic search have demonstrated greater robustness [23].

To further enhance generalization across diverse scenarios, HOPE proposed a hybrid policy that integrates RL with geometric constraints, ensuring that policies are informed with kinematic feasibility and are capable of executing complex multi-maneuver parking [8].

Despite their differences, these methods typically have limited success rate in confined-space parking. Both IL- and RL-based methods fundamentally attempt to learn a direct mapping from observations to actions. However, when the underlying action distribution is highly complex and when precise maneuvers are required, these explicit modeling approaches often face challenges [7]. Due to inherent modeling inaccuracy that could come from machine learning errors, distributional variance, or imperfect value estimation [11, 24], the resulting trajectories may be inaccurate, leading to collisions or excessive corrective maneuvers. This, in turn, reduces both the efficiency and the overall success rate of parking.

B. Diffusion Policy

Diffusion models have recently demonstrated remarkable success across diverse domains [25], with diffusion policies emerging as a compelling alternative to explicit action modeling by formulating policy learning as a conditional denoising process that reconstructs structured trajectories from noisy inputs [7]. Building on this foundation, a range of extensions have been introduced, such as enhanced spatial representations [26], accelerated inference schemes for real-time control [27], guided diffusion processes for improved generation controllability [28], and self-supervised strategies that strengthen representation learning under data scarcity [29]. These developments underscore the flexibility of diffusion policies, yet they rely on imitation of training distributions without explicit mechanisms for exploration or reward-driven optimization, which constrains their effectiveness in long-horizon decision-making [30].

Given the strong sequential decision-making capability of reinforcement learning (RL), recent research has explored integrating RL with diffusion [31]. RL introduces reward-driven objectives that complement the generative strengths of diffusion models, enabling policies to go beyond imitation and actively optimize for higher returns [32]. One category of work achieves this through reject sampling, where Q-values are used to filter action candidates generated by a behavior cloning diffusion policy [33, 34]. Another category employs weighted behavior cloning, reweighting diffusion-generated samples according to Q-values [35, 36]. While conceptually straightforward, these methods often suffer from low efficiency or remain limited in improving policy expressivity [12]. An alternative approach is to integrate diffusion models into reparameterized policy gradient methods, treating the diffusion policy as the actor and optimizing it directly with RL objectives [37]. Although this enables direct reward optimization, it relies on backpropagation through time (BPTT), which can introduce training instability and lead to suboptimal action choices [10]. In safety-critical tasks such as parking path planning, these limitations may ultimately reduce overall planning success rates.

In contrast to existing approaches, our setting leverages a pre-trained RL policy that already provides a reliable prior over actions. Rather than first pretraining a policy with IL and subsequently fine-tuning it with RL, we directly fine-tune the RL-pretrained policy through diffusion training, which could be in either an IL- or RL-based paradigm. This design not only refines the action distribution but also bypasses lengthy denoising procedures.

III. PRELIMINARIES

A. Problem Formulation

The parking path planning can be formulated as a sequential decision-making problem. At each discrete time step t , the vehicle pose is denoted by $P_t = (x_t, y_t, \theta_t)$, where (x_t, y_t) is the rear-axle center position and θ_t is the heading angle. The state is denoted as $s_t = E(P_t)$, which represents the environmental information obtained at pose P_t , including the target parking configuration, the occupancy map, and surrounding obstacles. Based on s_t , the policy π_θ generates an action

$$a_t \sim \pi_\theta(\cdot | s_t), \quad (1)$$

where $a_t = (v_t, \delta_t)$ consists of the vehicle's velocity $v_t \in [v_{\min}, v_{\max}]$ and steering angle $\delta_t \in [\delta_{\min}, \delta_{\max}]$.

The vehicle dynamics follow the kinematic model [38], yielding a deterministic transition function $f : \mathbb{R}^3 \times \mathbb{R}^2 \rightarrow \mathbb{R}^3$:

$$P_{t+1} = f(P_t, a_t) = \left(x_t + v_t \cos \theta_t \Delta t, y_t + v_t \sin \theta_t \Delta t, \theta_t + \frac{v_t}{L} \tan \delta_t \Delta t \right), \quad (2)$$

where L is the wheelbase and Δt is the discretization interval.

Overall, the parking path-planning task aims to learn a policy π_θ that generates a feasible trajectory from an initial vehicle pose P_0 to a target parking configuration P_T . A trajectory is represented as

$$\tau = (P_0, P_1, \dots, P_T), \quad (3)$$

and evolves according to

$$P_{t+1} = f(P_t, a_t), \quad a_t \sim \pi_\theta(\cdot | s_t), \quad s_t = E(P_t). \quad (4)$$

The terminal step T is defined as the first time the vehicle reaches a state sufficiently close to the target configuration.

The learned policy is therefore required to generate collision-free trajectories that respect vehicle kinematics and safety constraints. Learning such a policy can be approached in two mainstream ways. *Imitation learning (IL)* minimizes the discrepancy between the learned policy π_θ and an expert policy π^* , often through behavior cloning:

$$\min_{\theta} \mathbb{E}_{(s, a) \sim \mathcal{D}} [\ell(\pi_\theta(a | s), \pi^*(a | s))], \quad (5)$$

where \mathcal{D} is a dataset of expert demonstrations and $\ell(\cdot)$ is a loss function measuring the difference between the learned and expert actions. *Reinforcement learning (RL)* optimizes the policy π_θ by maximizing the expected discounted return with discount factor $\gamma \in (0, 1]$:

$$\theta^* = \arg \max_{\theta} \mathbb{E}_{\tau \sim \pi_\theta} \left[\sum_{t=0}^T \gamma^t r(s_t, a_t) \right], \quad (6)$$

where $r(s_t, a_t)$ denotes the reward signal obtained after executing action a_t at state s_t .

B. Diffusion Policy Preliminaries

A diffusion policy models a conditional distribution over actions given the state by denoising from noise to a clean action. Let $a^{(0)}$ denote the ground-truth action paired with observation o at state s . To avoid confusion, throughout this subsection we suppress the planning-time subscript (e.g., a_t, s_t) and simply write a, s, o . The diffusion (de/noising) timestep is indexed by a superscript $k \in \{0, \dots, K\}$, i.e., $a^{(k)}$ denotes the action at diffusion step k .

During training, a forward diffusion process progressively perturbs $a^{(0)}$ into a sequence $\{a^{(k)}\}_{k=1}^K$ under a variance schedule $\{\beta^k\}_{k=1}^K \subset (0, 1)$ with $\alpha^k := 1 - \beta^k$, $\bar{\alpha}^k := \prod_{i=1}^k \alpha^i$ [25]. In practice, β^k is typically chosen to increase with k (e.g., linear or cosine schedules), so that α^k and $\bar{\alpha}^k$ decrease monotonically as noise accumulates.

The step-wise forward (noising) kernel is

$$q(a^{(k)} | a^{(k-1)}) = \mathcal{N}(\sqrt{\alpha^k} a^{(k-1)}, \beta^k \mathbf{I}), \quad k = 1, \dots, K, \quad (7)$$

which yields the marginal closed form

$$a^{(k)} = \sqrt{\bar{\alpha}^k} a^{(0)} + \sqrt{1 - \bar{\alpha}^k} \epsilon, \quad \epsilon \sim \mathcal{N}(0, \mathbf{I}). \quad (8)$$

The reverse (denoising) process recovers $a^{(0)}$ from $a^{(K)} \sim \mathcal{N}(0, \mathbf{I})$ by iteratively reducing noise, using a neural network $\epsilon_\theta(a^{(k)}, k, o)$ that predicts the noise in $a^{(k)}$ given the timestep k and observation o observed at state s . In the Denoising Diffusion Probabilistic Model (DDPM) [25], the reverse transition is Gaussian:

$$p_\theta(a^{(k-1)} | a^{(k)}, o) = \mathcal{N}(\mu_\theta(a^{(k)}, k, o), \tilde{\beta}^k \mathbf{I}), \quad (9)$$

with mean

$$\mu_\theta(a^{(k)}, k, o) = \frac{1}{\sqrt{\alpha^k}} \left(a^{(k)} - \frac{\beta^k}{\sqrt{1 - \bar{\alpha}^k}} \epsilon_\theta(a^{(k)}, k, o) \right), \quad (10)$$

and variance

$$\tilde{\beta}^k = \frac{1 - \bar{\alpha}^{k-1}}{1 - \bar{\alpha}^k} \beta^k. \quad (11)$$

Based on DDPM, the Denoising Diffusion Implicit Model (DDIM) [39] shares the same forward process but improves the reverse update that preserves desired marginals while allowing fewer denoising steps. Defining the predicted clean action

$$\hat{a}^{(0)}(a^{(k)}, k, o) = \frac{a^{(k)} - \sqrt{1 - \bar{\alpha}^k} \epsilon_\theta(a^{(k)}, k, o)}{\sqrt{\alpha^k}}, \quad (12)$$

the non-stochastic DDIM update can be written as:

$$\hat{a}^{(k-1)} = \sqrt{\bar{\alpha}^{k-1}} \hat{a}^{(0)}(a^{(k)}, k, o) + \sqrt{1 - \bar{\alpha}^{k-1}} \epsilon_\theta(a^{(k)}, k, o), \quad (13)$$

Both DDPM and DDIM commonly adopt the same noise-prediction training objective by sampling $k \sim \mathcal{U}\{1, \dots, K\}$ and $\epsilon \sim \mathcal{N}(0, \mathbf{I})$:

$$\mathcal{L}_{\text{DP}}(\theta) = \mathbb{E}_{(a^{(0)}, o), k, \epsilon} \left[\|\epsilon - \epsilon_\theta(a^{(k)}, k, o)\|_2^2 \right]. \quad (14)$$

In this paper, we adopt the DDIM method. At inference, the diffusion policy conditions on s and executes the denoising process, initializing at $a^{(K)} \sim \mathcal{N}(0, \mathbf{I})$ and applying the update for $k = K, \dots, 1$ to obtain $a^{(0)}$.

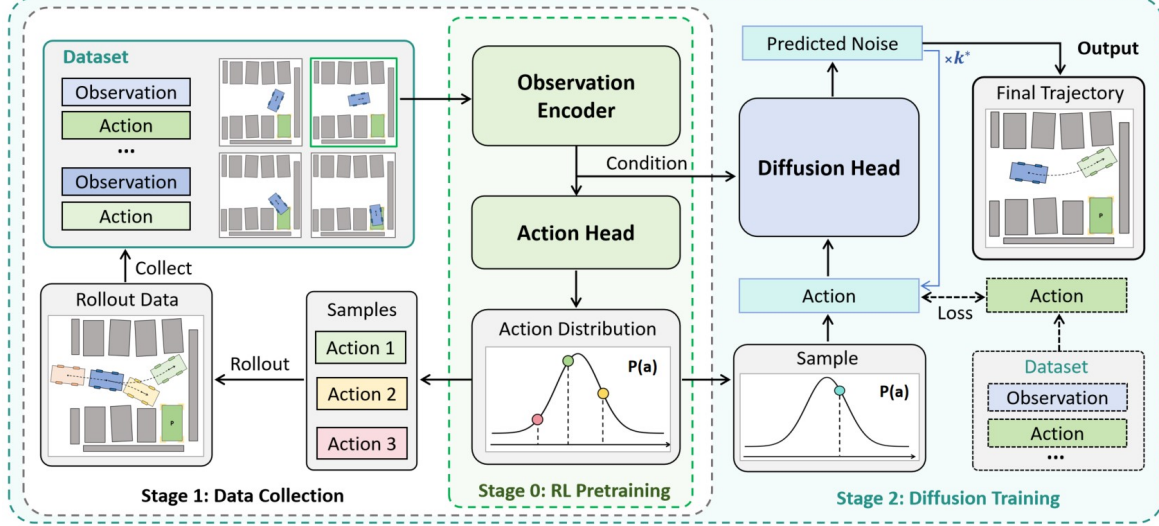


Fig. 2: Overview of the proposed framework: (1) pretrain an RL policy to obtain a state-conditional prior distribution; (2) rollout this policy to collect a dataset; (3) train a diffusion policy on the collected dataset to refine the prior (via IL or RL).

IV. METHODOLOGY

A. Diffusion-refinement Framework

We adopt a diffusion-refined RL framework that starts from a pretrained policy $\pi_{\text{RL}}(a|o)$ mapping observations to actions. In practice, π_{RL} is implemented with an observation encoder f_ϕ that extracts a latent representation $h = f_\phi(o)$, followed by a lightweight action head that outputs an explicit parametric action distribution, typically a Gaussian $\mathcal{N}(\mu_{\text{RL}}(o), \sigma_{\text{RL}}^2(o))$. While such explicit action modeling is effective in many settings, we observe that in confined parking scenarios, it can underfit the target action distribution. The mismatch may stem from biases inherent to explicit parameterizations or from imperfect value estimation during RL training [11]. Consequently, sampling from $\pi_{\text{RL}}(a|o)$ can occasionally yield suboptimal actions that cause collisions or induce unnecessary corrective maneuvers, degrading overall planning success.

To improve distributional fidelity without discarding existing RL knowledge, we adopt a self-distillation-style refinement pipeline. We first rollout the pretrained policy $\pi_{\text{RL}}(a|o)$ in the environment, sampling actions from $\mathcal{N}(\mu_{\text{RL}}(o), \sigma_{\text{RL}}^2(o))$ and recording trajectories. Rollouts that reach the target configuration within a prescribed interaction step budget and remain collision-free are retained as successful demonstrations, while trajectories exceeding the budget are discarded. The resulting set of successful observation-action pairs serves as training data for diffusion refinement, allowing us to retain the strengths of π_{RL} while filtering out its failure modes.

We then augment the pretrained architecture with a diffusion head to refine actions around the RL prior. The encoder f_ϕ is reused to provide conditioning $h = f_\phi(o)$ to a denoising network $\epsilon_\theta(a^{(k)}, k, o)$, where $k \in \{0, \dots, K\}$ indexes the diffusion (de/noising) step. Unlike standard diffusion policies that initialize from a standard Gaussian $a^{(K)} \sim \mathcal{N}(0, \mathbf{I})$, we initialize from the RL prior $a^{(k)} \sim \mathcal{N}(\mu_{\text{RL}}(o), \sigma_{\text{RL}}^2(o))$ for some $k < K$ and perform a short reverse denoising chain to obtain a refined action $a^{(0)}$. During diffusion training, pairs

(o, a) are sampled from the collected demonstration set, and the action serves as the clean target $a^{(0)}$. Overall, this design leverages π_{RL} as a structured prior and tasks the diffusion module with distributional refinement to sharpen and correct the RL outputs precisely in a confined space.

B. Prior-Aligned Diffusion

When deploying the planner, we initialize the reverse (denoising) process from the pretrained RL prior and execute only the last k denoising steps for some truncation index k . However, under standard diffusion training, the marginal at an intermediate step k follows the forward relation in Eq. (8), whose mean depends on $a^{(0)}$ and whose standard deviation equals $\sqrt{1 - \bar{\alpha}^k}$. As shown in Fig. 3, this does *not* match the RL prior:

$$p_{\text{RL}}(a | o) = \mathcal{N}(\mu_{\text{RL}}(o), \sigma_{\text{RL}}^2(o)), \quad (15)$$

which creates a distributional mismatch at the truncation point and induces biased denoising updates, ultimately degrading action accuracy. To ensure training-inference consistency, we therefore modify the noising procedure during training so that the reverse trajectory is *prior-aligned*. For clarity, we omit the observation o in the derivations below (all quantities are conditioned on o unless stated otherwise).

1) *Introduction of Time-Variant Mean:* We desire the truncated initialization $a^{(k^*)}$ to match the RL prior in Eq. (15) for some $k^* < K$, so that inference can start at $k = k^*$ rather than from pure noise. To this end, we replace the standard forward parameterization (as shown in Eq. (8)) with a prior-centered mean schedule:

$$a^{(k)} = \sqrt{\bar{\alpha}^k} \mu(k) + \sqrt{1 - \bar{\alpha}^k} \epsilon, \quad \epsilon \sim \mathcal{N}(0, \mathbf{I}), \quad (16)$$

where $\mu(k)$ is a k -dependent mean to be designed. The truncation index k^* is selected to match the standard deviation of $a^{(k)}$ to that of the RL prior:

$$k^* = \arg \min_k |\sigma_{\text{RL}} - \sqrt{1 - \bar{\alpha}^k}|. \quad (17)$$

Training–inference consistency further requires that the mean schedule reproduce the correct marginals at the endpoints:

$$\begin{aligned}\mathbb{E}[a^{(0)}] &= \sqrt{\bar{\alpha}^0} \mu(0) = a^{(0)}, \\ \mathbb{E}[a^{(k^*)}] &= \sqrt{\bar{\alpha}^{k^*}} \mu(k^*) = \sqrt{\bar{\alpha}^{k^*}} \mu_{\text{RL}}.\end{aligned}\quad (18)$$

We parameterize the schedule as a two-term interpolation,

$$\mu(k) = w_1(k) \mu_{\text{RL}} + w_2(k) a^{(0)}, \quad (19)$$

and constrain the weights to satisfy Eq. (18); in particular,

$$w_1(k^*) = w_2(0) = 1, \quad w_1(0) = w_2(k^*) = 0. \quad (20)$$

A concrete schedule for (w_1, w_2) will be specified in Sec. *Selection of Coefficients*, where we additionally ensure numerically stable scaling of the training loss near small k .

2) *Training Objective*: With the time-variant mean $\mu(k)$, the forward (noising) process in Eq. (16) can be rewritten as

$$\begin{aligned}a^{(k)} &= \sqrt{\bar{\alpha}^k} \mu(k) + \sqrt{1 - \bar{\alpha}^k} \epsilon \\ &= \sqrt{\bar{\alpha}^k} a^{(0)} + \sqrt{1 - \bar{\alpha}^k} \left(\sqrt{\frac{\bar{\alpha}^k}{1 - \bar{\alpha}^k}} [\mu(k) - a^{(0)}] + \epsilon \right).\end{aligned}\quad (21)$$

Comparing with Eq. (8), the corresponding noise-prediction objective becomes

$$\mathcal{L}_{\text{DP}}(\theta) = \mathbb{E}_{a^{(0)}, k, \epsilon} \left[\left\| \epsilon + \sqrt{\frac{\bar{\alpha}^k}{1 - \bar{\alpha}^k}} (\mu(k) - a^{(0)}) - \epsilon_{\theta}(a^{(k)}, k) \right\|_2^2 \right]. \quad (22)$$

This indicates that during training the Gaussian perturbation $\epsilon \sim \mathcal{N}(0, \mathbf{I})$ is applied around the scheduled mean $\mu(k)$ rather than the clean action $a^{(0)}$.

3) *Selection of Coefficients*: A direct concern in Eq. (22) is the factor $\sqrt{\bar{\alpha}^k}/(1 - \bar{\alpha}^k)$, which can become large as $k \rightarrow 0$. To stabilize learning, we choose (w_1, w_2) so that the terms coupled with $1/\sqrt{1 - \bar{\alpha}^k}$ remain bounded. Using Eqs. (19) and (18),

$$\begin{aligned}\sqrt{\frac{\bar{\alpha}^k}{1 - \bar{\alpha}^k}} [\mu(k) - a^{(0)}] &= \\ w_1(k) \sqrt{\frac{\bar{\alpha}^k}{1 - \bar{\alpha}^k}} \mu_{\text{RL}} - (1 - w_2(k)) \sqrt{\frac{\bar{\alpha}^k}{1 - \bar{\alpha}^k}} a^{(0)} &= (23)\end{aligned}$$

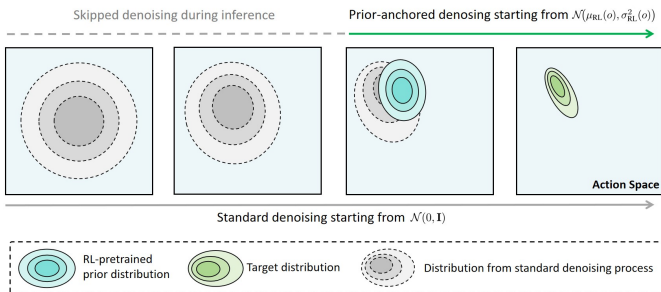


Fig. 3: Illustration for the proposed prior-aligned diffusion training. Standard diffusion starts from random noise and yields an intermediate distribution that does not align with the RL-pretrained prior distribution. Our goal is to match the distribution from the denoising process with the prior distribution through alignment training, so the denoising process can start from the prior distribution at inference.

Algorithm 1 Training Procedure

Require: Pretrained $\pi_{\text{RL}}(a | o)$, dataset \mathcal{D} from π_{RL} rollouts; schedule $\{\beta^k\}_{k=1}^K$ and $\{\alpha^k\}_{k=1}^K$; learning rate η

- 1: Initialize diffusion head ϵ_{θ}
- 2: Initialize critic network \tilde{Q}_{ψ} (Only offline RL)
- 3: Calculate truncation step k^* via Eq. (17)
- 4: **for** Iteration $i = 1$ to N **do**
- 5: Sample $(o, a^{(0)}) \sim \mathcal{D}$, $k \sim \text{Unif}\{1, \dots, K\}$
- 6: Form RL prior $\mathcal{N}(\mu_{\text{RL}}(o), \sigma_{\text{RL}}^2(o))$ with $\pi_{\text{RL}}(a | o)$
- 7: Build $\mu(k)$ using Eq. (26)
- 8: Form $a^{(k)}$ by adding noise to $\mu(k)$ using Eq. (16)
- 9: Predict the noise $\epsilon_{\theta}(a^{(k)}, k, o)$
- 10: Compute $\mathcal{L}_{\text{DP}}(\theta)$ by Eq. (22)
- 11: **if** Offline RL **then**
- 12: **for** $k = k^*$ to 1 **do**
- 13: Predict action $\hat{a}^{(k-1)}$ using Eqs. (12) and (13)
- 14: **end for**
- 15: Set $\mathcal{L}(\theta) \leftarrow \mathcal{L}_{\text{DP}}(\theta) - \lambda \tilde{Q}_{\psi}(o, \hat{a}^{(0)})$ (cf. Eq. (27))
- 16: **else**
- 17: Set $\mathcal{L}(\theta) \leftarrow \mathcal{L}_{\text{DP}}(\theta)$
- 18: **end if**
- 19: Update $\theta \leftarrow \theta - \eta \nabla_{\theta} \mathcal{L}(\theta)$
- 20: **end for**

Since μ_{RL} , $a^{(0)}$, and $\sqrt{\bar{\alpha}^k}$ are bounded, the only potentially unbounded factors in Eq. (23) come from the ratios $w_1(k)/\sqrt{1 - \bar{\alpha}^k}$ and $(w_2(k) - 1)/\sqrt{1 - \bar{\alpha}^k}$. Therefore, it suffices to impose the bounds

$$\left| \frac{w_1(k)}{\sqrt{1 - \bar{\alpha}^k}} \right| \leq U, \quad \left| \frac{1 - w_2(k)}{\sqrt{1 - \bar{\alpha}^k}} \right| \leq U, \quad (24)$$

for some constant $U > 0$, together with the endpoint constraints in Eq. (18).

To meet these requirements, we choose a schedule that interpolates with the accumulated noise standard deviation:

$$\begin{aligned}w_1(k) &= \begin{cases} \sqrt{\frac{1 - \bar{\alpha}^k}{1 - \bar{\alpha}^{k^*}}}, & k \leq k^*, \\ 1, & k > k^*, \end{cases} \\ w_2(k) &= \begin{cases} 1 - \sqrt{\frac{1 - \bar{\alpha}^k}{1 - \bar{\alpha}^{k^*}}}, & k \leq k^*, \\ 0, & k > k^*. \end{cases}\end{aligned}\quad (25)$$

This schedule satisfies the requirements in Eqs. (18) and (20). Moreover, Eq. (24) holds with $U = 1/\sqrt{1 - \bar{\alpha}^{k^*}}$. In practice, U remains moderate; for example, under a typical cosine noise schedule and $k^* = K/5$, one often has $U \approx 3$. The resulting (w_1, w_2) are monotone in k , yield a smooth interpolation from $a^{(0)}$ to μ_{RL} , and guarantee numerically stable scaling of the training objective near $k \rightarrow 0$.

Algorithm 2 Inference Procedure

Require: Observation o , truncation index k^*

- 1: Form RL prior $\mathcal{N}(\mu_{\text{RL}}(o), \sigma_{\text{RL}}^2(o))$ with $\pi_{\text{RL}}(a | o)$
- 2: Sample $a^{(k^*)} \sim \mathcal{N}(\mu_{\text{RL}}(o), \sigma_{\text{RL}}^2(o))$
- 3: **for** $k = k^*$ **to** 1 **do**
- 4: Predict the noise $\epsilon_\theta(a^{(k)}, k, o)$
- 5: Obtain action $\hat{a}^{(k-1)}$ using Eqs. (12) and (13)
- 6: **end for**
- 7: Output $\hat{a}^{(0)}$

C. Training–Inference Pipeline and Learning Objectives

Using Eqs. (19) and (25), the time-variant mean $\mu(k)$ is fully specified as

$$\mu(k) = \begin{cases} \sqrt{\frac{1-\bar{\alpha}^k}{1-\bar{\alpha}^{k^*}}} \mu_{\text{RL}} + \left(1 - \sqrt{\frac{1-\bar{\alpha}^k}{1-\bar{\alpha}^{k^*}}}\right) a^{(0)}, & k \leq k^* \\ \mu_{\text{RL}}, & k > k^* \end{cases} \quad (26)$$

and the prior-aligned forward process in Eq. (16) yields the diffusion imitation-learning loss in Eq. (22).

Note that our use of RL at the first stage is purely pretraining (to provide a structured prior and rollouts). This usage is orthogonal to prior work that optimizes diffusion with RL, which means our method can be seamlessly augmented with existing offline diffusion RL training approaches. We retain \mathcal{L}_{DP} as a BC regularizer and add a value-maximization term evaluated on the final action produced by the truncated DDIM reverse chain shown in Eqs. (12) and (13). Concretely, starting from $a^{(k^*)} \sim \mathcal{N}(\mu_{\text{RL}}, \sigma_{\text{RL}}^2)$, we apply the deterministic DDIM updates for $k = k^*, \dots, 1$ and denote the final action by $\hat{a}^{(0)}$. Let $\tilde{Q}_\psi(o, a)$ denote a value estimator that could either be a single critic $Q_\psi(o, a)$ or the minimum over twin critics $\min\{Q_{\psi_1}(o, a), Q_{\psi_2}(o, a)\}$ in practice, the diffusion–offline RL objective (in the spirit of diffusion Q-learning [40]) is

$$\mathcal{L}_{\text{DQL}}(\theta) = \mathcal{L}_{\text{DP}}(\theta) - \lambda \mathbb{E}_{o, a^{(k^*)} \sim \mathcal{N}(\mu_{\text{RL}}, \sigma_{\text{RL}}^2)} \left[\tilde{Q}_\psi(o, \hat{a}^{(0)}) \right], \quad (27)$$

where $\lambda > 0$ is a coefficient to balance BC regularization and value maximization.

Overall, the training procedure is summarized in Alg. 1, where the forward (noising) process and the objective are modified to align diffusion training with the RL prior. At inference, as shown in Alg. 2, we initialize from the RL prior and run a truncated reverse denoising chain to obtain the final action $\hat{a}^{(0)}$.

V. EXPERIMENT

A. Experimental Setup

We evaluate our method on the HOPE benchmark [8], which composes diverse parking scenes from the open-source DLP dataset and a 2D simulator [41, 42]. Scenarios are categorized into three difficulty levels, *normal*, *medium*, and *hard*, according to spatial narrowness following ISO 20900 [43]. Our training scenes includes 2,000 hard-level scenes, 3,000 medium-level scenes, and 2,000 normal-level scenes. In total, we use 7,000 scenes for training, 700 for validation, and another 700 for testing. From the pretrained RL policy

rollouts discussed in Sec. IV-A, we collect 158,706 successful state–action pairs from the 7,000 training scenes for the diffusion training. For the experiment results, each testing scene is repeated 10 times, and the average success rate is taken to obtain the final success rate for each difficulty level and the overall success rate.

At evaluation time, each episode is limited to 50 interaction steps. Failing to reach the target configuration within this budget is counted as a planning failure. For fairness, all methods enable *analytic expansions* [15], a shortcut practice commonly used in unstructured planning. We report planning *success rate* on the 700-scene test set and also break down results by difficulty.

Following the benchmark, the observation at each step comprises: (i) an ego-centered bird’s-eye-view (BEV) occupancy raster in which occupied cells (obstacles, boundaries, parked vehicles) are 1 and drivable are 0; (ii) radial obstacle distances sampled every 10°, and (iii) the relative parking-slot configuration in the ego frame (position, heading, and slot orientation). The action space is two-dimensional, and each step outputs a path increment (step length) and a steering command.

All learning-based baselines and our approach share the same observation encoder, a pretrained transformer-based module that produces a 512-D representation [8]. We then use this feature as the diffusion condition, followed by either an action head (for explicit models) or a diffusion head that outputs the 2-D action.

Training and optimization hyperparameters are summarized in Table I. All diffusion-based methods use the same $\{\beta^k\}_{k=1}^K$ schedule and accumulated products $\{\bar{\alpha}^k\}_{k=1}^K$, and the truncation index k^* is selected by Eq. (17). Experiments are carried out on a single NVIDIA RTX-3090 and a 32-core AMD EPYC 7542 CPU.

B. Experiment Results

We compare against a widely used non-learning planning method and planners trained with learning-based methods.

- **Hybrid A*.** A non-learning heuristic search planner widely used for unstructured planning. It is designed to consider the vehicle’s non-holonomic constraints and uses analytic expansions to connect feasible motion primitives.

TABLE I: Key hyperparameters.

Hyperparameter	Value
RL pretrain episodes	100,000
Diffusion epochs	60
Training batch size	64
Optimizer	AdamW
Diffusion learning rate	1×10^{-4}
Encoder learning rate	1×10^{-5}
DDIM train steps	100
DDIM inference steps	25
Truncation step k^*	5
DDIM β^k range	[0.0001, 0.02]
Noise schedule	Cosine
RL discount γ	0.98
DQL weight λ	1

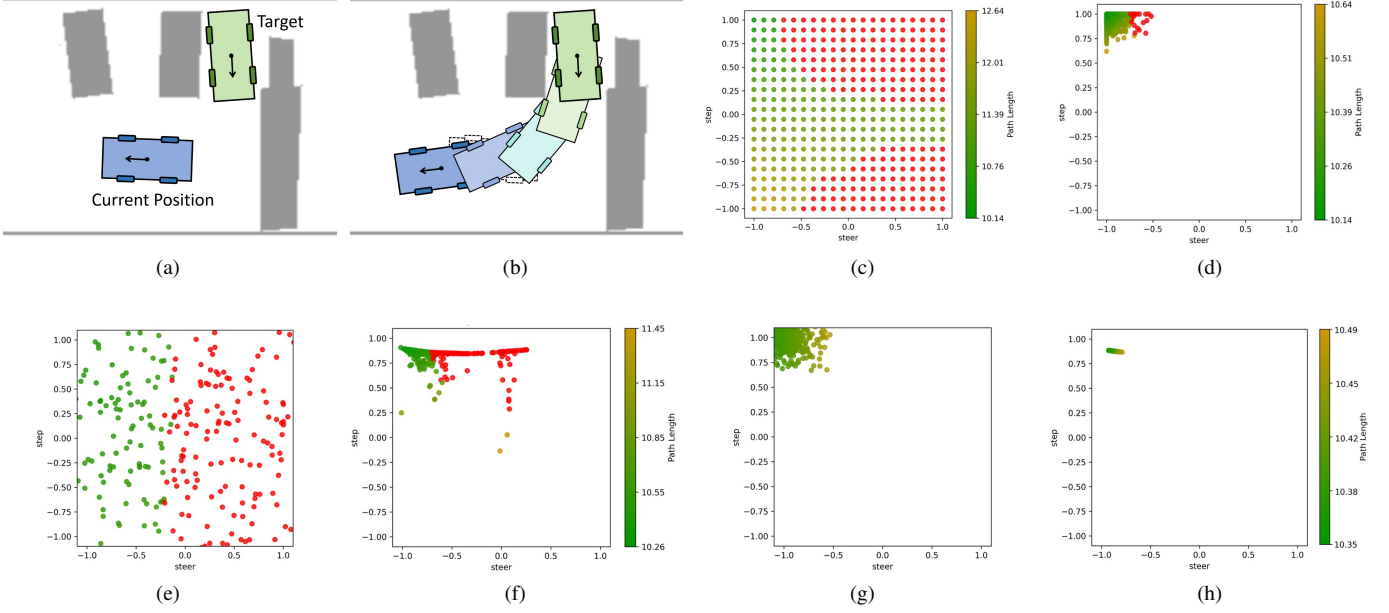


Fig. 4: Visualization for a vertical parking scenario. (a) Scene overview. (b) A reasonable path planning for one-time park-in. (c) Feasibility of 400 uniformly sampled actions in the local action space; actions enabling a single-maneuver park-in with one gear change are highlighted in green/yellow. Others are in red. (d) RL-pretrained action distribution at the same position. (e) Random action initialization from diffusion policy before denoising. (f) Action distribution with diffusion policy after denoising. (g) Proposed diffusion refinement initialized from the RL-pretrained prior distribution; (h) Final action distribution after prior-aligned denoising.

TABLE II: Average success rate (%) under different parking scenario difficulties.

Paradigm	Method	Hard	Medium	Normal	Avg.
/	HA*	6.0	74.3	82.5	57.1
Pretrain (RL)	PPO	28.8	81.6	83.8	67.1
	SAC	43.2	85.5	92.9	75.5
Diffusion (IL)	DP	48.3	85.2	92.7	76.8
	+ RL init.	46.6	88.5	91.4	77.4
	DRIP (ours)	59.1	88.9	96.2	82.4
Diffusion (RL)	DQL	45.0	86.4	91.0	75.9
	+ RL init.	51.0	89.0	94.4	79.7
	DRIP (ours)	65.9	92.0	96.8	85.9

- **Reinforcement Learning (RL).** Following the HOPE training protocol [8], we apply two planners, an on-policy **PPO**-based planner and an off-policy **SAC**-based planner. These serve both as competitive baselines and as the source of pretrained policies used for parameter initialization in diffusion-based methods.
- **Diffusion Policy (DP)** [7]. A diffusion planner that models the policy via conditional denoising and is trained with imitation learning. We apply the version (**DP**), which is trained from scratch using the IL objective (Eq. (14)) as applied in the original paper, and the variant (**+ RL init.**), which shares the same training process but initializes the encoder backbone using RL-pretrained parameters.
- **Diffusion Q-Learning (DQL)** [40]. A diffusion actor optimized with an offline RL objective. We also report

two versions of this method. The approach (**DQL**), as applied in the original paper, uses the Q-learning loss with behavior cloning regularization (Eq. (27)) without RL pretraining, and the version (**+ RL init.**) initializes the encoder backbone with RL-pretrained parameters.

- **Diffusion Refined Planner (DRIP).** Our prior-aligned diffusion refinement framework that (i) *starts* the reverse process from the pretrained RL-pretrained prior distribution at a truncation step, and (ii) *aligns* the training forward process to that prior via the proposed prior-alignment training process. We evaluate our methods trained under both the imitation-learning paradigm (IL) and the reinforcement learning paradigm (RL). In both cases, the backbone is initialized from the pretrained RL policy, while the diffusion head is trained with our prior-aligned scheme.

Table II reports success rates for the above methods. Hybrid A* exhibits low success on hard cases and modest performance overall, whereas RL-pretrained agents attain better success across difficulty levels, indicating the benefit of data-driven learning. Similarly, DP and DQL achieve performance comparable to RL baselines, but performance gains are limited when trained from scratch. This indicates that learning to denoise from pure noise without an informative prior is challenging in a confined space configuration. Initializing from an RL-pretrained policy improves the diffusion baselines slightly by **+0.6%** for DP and **+3.8%** for DQL, with the larger gain for DQL plausibly due to better alignment between the RL-style objective used in both pretraining and the second-stage

diffusion training.

In contrast, our Diffusion Refinement approach yields consistent and substantial improvements. Relative to their RL-initialized counterparts, **DRIP** improves overall success by **+5.0%** and **+6.2%**, respectively. Compared to training from scratch, the gains are **+5.6%** (over DP) and **+10.0%** (over DQL). Improvements are most pronounced on *hard* scenes, with a gain of **+10.8%** over DP and **+10.9%** over DQL. These results support the effectiveness of our proposed diffusion-based refinement method, not mere parameter initialization, for learning a better policy in confined-space parking.

We illustrate the effect of the proposed method with a case study in a vertical parking scene shown in Fig. 4. As shown in Fig. 4 (a,b), a reasonable strategy is to move forward left and then the vehicle can complete parking with at most a single gear change. Actions that steer forward right, by contrast, often make a one-switch maneuver impossible, even at maximum steering the vehicle collides or becomes trapped by obstacles. To make this constraint explicit, we uniformly sample 400 actions in the local action space (step length, steering) and, for each action, check whether the post-action pose can be connected to the target slot by a Reeds–Shepp (RS) maneuver with one gear change [44]. Feasible actions are colored yellow/green in Fig. 4 (c), where greener indicates a shorter remaining path, while infeasible ones are red. The “good” actions concentrate in a narrow band in the upper-left region of the action space.

We then visualize three policies in the same position. The pretrained RL policy (Fig. 4 (d)) captures the overall structure of the feasible action distribution but still includes a nontrivial probability of suboptimal actions (about 4% infeasible/red in this case), reflecting the limits of explicit distribution modeling. A standard diffusion policy initialized from pure noise (Fig. 4 (e,f)) tends to denoise in the general direction towards the feasible band but struggles to concentrate probability within the green region. In contrast, our diffusion refinement starts denoising from the RL prior (Fig. 4 (g)). With prior-aligned training, it can concentrate the final distribution within the feasible band (Fig. 4 (h)), yielding a more precise action model for this confined scenario.

C. Ablation Study.

We evaluate the effect of the proposed prior-aligned training process. As shown in Tab. III, directly using the RL-pretrained distribution as the initialization for truncated diffusion *without* alignment performs suboptimally relative to the corresponding DP/DQL baselines, and success rates exhibit slight drops. The reason is that, at the truncation step, the marginal of a standard diffusion process does not match the RL-pretrained distribution. Starting denoising from this mismatched prior leads to biased updates. In contrast, applying the proposed alignment during training yields consistent and significant improvements in success rate.

We select the truncation step k^* by Eq. (17), i.e., the step whose standard-diffusion variance $\sqrt{1 - \bar{\alpha}^k}$ is closest to the RL prior’s standard deviation σ_{RL} . In practice, with our pretrained policy and noise schedule, this gives $k^*/K \approx 0.2$;

TABLE III: Ablation on prior-aligned training and truncation ratio k^*/K .

Method	k^*/K	Hard	Medium	Normal	Avg.
Diffusion (IL)					
DP	1.0	48.3	85.2	92.7	76.8
Prior init. only	0.2	46.0	85.8	91.8	76.1
DRIP	0.1	52.1	86.6	92.8	78.5
DRIP (ours)	0.2	59.1	88.9	96.2	82.4
DRIP	0.4	46.8	83.4	88.8	74.5
Diffusion (RL)					
DQL	1.0	45.0	86.4	91.0	75.9
Prior init. only	0.2	37.4	83.1	90.5	72.1
DRIP	0.1	61.3	91.2	96.1	84.0
DRIP (ours)	0.2	65.9	92.0	96.8	85.9
DRIP	0.4	54.1	91.7	94.6	81.8

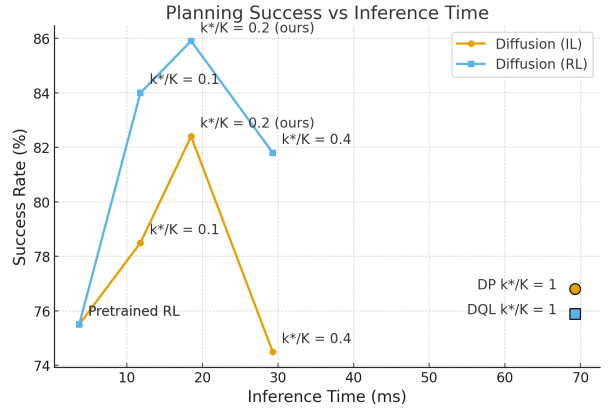


Fig. 5: Comparison of average planning success rate (%) and inference time (ms) between different methods.

with 25 inference steps, this corresponds to $k^* = 0.2 \times 25 = 5$. Tab. III and Fig. 5 also report results for alternative ratios k^*/K . Both smaller and larger values degrade performance. Fewer denoising steps under-refine the action distribution, whereas more steps inject excessive noise that dilutes the prior. Besides, the selection of $k^*/K = 0.2$ achieves the best performance, with a single-step inference time of 18.5 ms. This corresponds to a successful autoregressive generation of a full trajectory within one second, assuming the maximum number of steps is set to 50. These observations further highlight the necessity of distributional alignment at the truncation point.

VI. CONCLUSION AND FUTURE WORK

This work presented a *diffusion-refined reinforcement learning (RL) planner* for confined-space parking. Motivated by the observation that explicit action modeling often fails to accurately capture the complex, precision-critical action distributions required in narrow spaces under non-holonomic constraints, we propose a method to refine the action distribution with diffusion training. We first pretrain a policy with RL to provide a structured prior over actions and then refine this prior distribution with a diffusion model. One technical challenge is that standard diffusion training produces intermediate marginals whose mean/variance generally do not

match the pretrained prior at the truncation point, creating a training-inference mismatch when we initialize inference from the pretrained distribution. To resolve this, we introduced a prior-aligned training procedure that modifies the forward (noising) process with a time-variant mean, ensuring the denoising trajectory is distributionally aligned with the RL prior at a chosen step. This allows inference to start directly from the pretrained distribution and perform a short, well-informed denoising chain.

Across the parking benchmark, including *normal*, *medium*, and *hard* scenes, the proposed planner consistently refines the RL-pretrained action distribution and achieves higher planning success rates. Compared to diffusion policies trained without RL priors, our method also obtains significant performance gains, especially in the hard, most confined scenarios. Visualization and ablation further indicate that the improvement stems not only from using a prior distribution but critically from the proposed alignment, and mere parameter initialization is insufficient to realize these benefits.

An important extension of this work is to combine diffusion refinement with online RL. While our framework already integrates diffusion training cleanly with imitation learning and offline RL, the proposed method also has the potential to incorporate interactive rollouts and policy improvement in the loop. Promising directions include jointly learning the truncation step and noise schedule, updating the critic and prior under on-policy data to obtain higher success rates and better generalization.

REFERENCES

- [1] S. F. Franco, “Parking prices and availability, mode choice and urban form.” International Transport Forum Discussion Paper, 2020.
- [2] M. Khalid, K. Wang, N. Aslam, Y. Cao, N. Ahmad, and M. K. Khan, “From smart parking towards autonomous valet parking: A survey, challenges and future works,” *Journal of Network and Computer Applications*, vol. 175, p. 102935, 2021.
- [3] J. M. Kim, K. I. Lim, and J. H. Kim, “Auto parking path planning system using modified reeds-shepp curve algorithm,” in *2014 11th International Conference on Ubiquitous Robots and Ambient Intelligence (URAI)*. IEEE, 2014, pp. 311–315.
- [4] S. Sedighi, D.-V. Nguyen, and K.-D. Kuhnert, “Guided hybrid a-star path planning algorithm for valet parking applications,” in *2019 5th international conference on control, automation and robotics (ICCAR)*. IEEE, 2019, pp. 570–575.
- [5] A. Likmeta, A. M. Metelli, A. Tirinzoni, R. Giol, M. Restelli, and D. Romano, “Combining reinforcement learning with rule-based controllers for transparent and general decision-making in autonomous driving,” *Robotics and Autonomous Systems*, vol. 131, p. 103568, 2020.
- [6] S. Teng, X. Hu, P. Deng, B. Li, Y. Li, Y. Ai, D. Yang, L. Li, Z. Xuanyuan, F. Zhu *et al.*, “Motion planning for autonomous driving: The state of the art and future perspectives,” *IEEE Transactions on Intelligent Vehicles*, 2023.
- [7] C. Chi, Z. Xu, S. Feng, E. Cousineau, Y. Du, B. Burchfiel, R. Tedrake, and S. Song, “Diffusion policy: Visuomotor policy learning via action diffusion,” *The International Journal of Robotics Research*, p. 02783649241273668, 2023.
- [8] M. Jiang, Y. Li, S. Zhang, S. Chen, C. Wang, and M. Yang, “Hope: A reinforcement learning-based hybrid policy path planner for diverse parking scenarios,” *IEEE Transactions on Intelligent Transportation Systems*, 2025.
- [9] Y. Wang, L. Wang, Y. Jiang, W. Zou, T. Liu, X. Song, W. Wang, L. Xiao, J. Wu, J. Duan *et al.*, “Diffusion actor-critic with entropy regulator,” *Advances in Neural Information Processing Systems*, vol. 37, pp. 54183–54204, 2024.
- [10] A. Z. Ren, J. Lidard, L. L. Ankile, A. Simeonov, P. Agrawal, A. Majumdar, B. Burchfiel, H. Dai, and M. Simchowitz, “Diffusion policy policy optimization,” *arXiv preprint arXiv:2409.00588*, 2024.
- [11] S. Park, K. Frans, S. Levine, and A. Kumar, “Is value learning really the main bottleneck in offline rl?” *Advances in Neural Information Processing Systems*, vol. 37, pp. 79029–79056, 2024.
- [12] S. Park, Q. Li, and S. Levine, “Flow q-learning,” *arXiv preprint arXiv:2502.02538*, 2025.
- [13] H. Zheng, Z. Zhou, G. Zhang, Z. Wang, K. Wang, P. Li, S. Shen, M. Yang, and T. Qin, “Multipark: Multimodal parking transformer with next-segment prediction,” *arXiv preprint arXiv:2508.11537*, 2025.
- [14] B. Li, T. Acarman, Y. Zhang, Y. Ouyang, C. Yaman, Q. Kong, X. Zhong, and X. Peng, “Optimization-based trajectory planning for autonomous parking with irregularly placed obstacles: A lightweight iterative framework,” *IEEE Transactions on Intelligent Transportation Systems*, vol. 23, no. 8, pp. 11970–11981, 2021.
- [15] D. Dolgov, S. Thrun, M. Montemerlo, and J. Diebel, “Path planning for autonomous vehicles in unknown semi-structured environments,” *The international journal of robotics research*, vol. 29, no. 5, pp. 485–501, 2010.
- [16] M. Czubenko, Z. Kowalcuk, and A. Ordys, “Autonomous driver based on an intelligent system of decision-making,” *Cognitive computation*, vol. 7, pp. 569–581, 2015.
- [17] B. R. Kiran, I. Sobh, V. Talpaert, P. Mannion, A. A. Al Sallab, S. Yogamani, and P. Pérez, “Deep reinforcement learning for autonomous driving: A survey,” *IEEE Transactions on Intelligent Transportation Systems*, vol. 23, no. 6, pp. 4909–4926, 2021.
- [18] R. Chai, D. Liu, T. Liu, A. Tsourdos, Y. Xia, and S. Chai, “Deep learning-based trajectory planning and control for autonomous ground vehicle parking maneuver,” *IEEE Transactions on Automation Science and Engineering*, 2022.
- [19] W. Liu, Z. Li, L. Li, and F.-Y. Wang, “Parking like a human: A direct trajectory planning solution,” *IEEE Transactions on Intelligent Transportation Systems*, vol. 18,

no. 12, pp. 3388–3397, 2017.

[20] C. Li, Z. Ji, Z. Chen, T. Qin, and M. Yang, “Parkinge2e: Camera-based end-to-end parking network, from images to planning,” in *2024 IEEE/RSJ International Conference on Intelligent Robots and Systems (IROS)*. IEEE, 2024, pp. 13 206–13 212.

[21] Z. Du, Q. Miao, and C. Zong, “Trajectory planning for automated parking systems using deep reinforcement learning,” *International Journal of Automotive Technology*, vol. 21, pp. 881–887, 2020.

[22] Z. Wang, Z. Chen, M. Jiang, T. Qin, and M. Yang, “Rl-ogm-parking: Lidar ogm-based hybrid reinforcement learning planner for autonomous parking,” *arXiv preprint arXiv:2502.18846*, 2025.

[23] J. Bernhard, R. Gieselmann, K. Esterle, and A. Knoll, “Experience-based heuristic search: Robust motion planning with deep q-learning,” in *2018 21st International conference on intelligent transportation systems (ITSC)*. IEEE, 2018, pp. 3175–3182.

[24] W. Zhang, Y. Feng, F. Meng, D. You, and Q. Liu, “Bridging the gap between training and inference for neural machine translation,” *arXiv preprint arXiv:1906.02448*, 2019.

[25] J. Ho, A. Jain, and P. Abbeel, “Denoising diffusion probabilistic models,” *Advances in neural information processing systems*, vol. 33, pp. 6840–6851, 2020.

[26] Y. Ze, G. Zhang, K. Zhang, C. Hu, M. Wang, and H. Xu, “3d diffusion policy: Generalizable visuomotor policy learning via simple 3d representations,” *arXiv preprint arXiv:2403.03954*, 2024.

[27] Z. Dong, J. Hao, Y. Yuan, F. Ni, Y. Wang, P. Li, and Y. Zheng, “Diffuserlite: Towards real-time diffusion planning,” *Advances in Neural Information Processing Systems*, vol. 37, pp. 122 556–122 583, 2024.

[28] M. T. Jackson, M. T. Matthews, C. Lu, B. Ellis, S. Whitenon, and J. Foerster, “Policy-guided diffusion,” *arXiv preprint arXiv:2404.06356*, 2024.

[29] X. Li, V. Belagali, J. Shang, and M. S. Ryoo, “Crossway diffusion: Improving diffusion-based visuomotor policy via self-supervised learning,” in *2024 IEEE International Conference on Robotics and Automation (ICRA)*. IEEE, 2024, pp. 16 841–16 849.

[30] M. Song, X. Deng, Z. Zhou, J. Wei, W. Guan, and L. Nie, “A survey on diffusion policy for robotic manipulation: Taxonomy, analysis, and future directions,” *Authorea Preprints*, 2025.

[31] Z. Zhu, H. Zhao, H. He, Y. Zhong, S. Zhang, H. Guo, T. Chen, and W. Zhang, “Diffusion models for reinforcement learning: A survey,” *arXiv preprint arXiv:2311.01223*, 2023.

[32] M. Janner, Y. Du, J. B. Tenenbaum, and S. Levine, “Planning with diffusion for flexible behavior synthesis,” *arXiv preprint arXiv:2205.09991*, 2022.

[33] H. Chen, C. Lu, C. Ying, H. Su, and J. Zhu, “Offline reinforcement learning via high-fidelity generative behavior modeling,” *arXiv preprint arXiv:2209.14548*, 2022.

[34] P. Hansen-Estruch, I. Kostrikov, M. Janner, J. G. Kuba, and S. Levine, “Idql: Implicit q-learning as an actor-critic method with diffusion policies,” *arXiv preprint arXiv:2304.10573*, 2023.

[35] C. Lu, H. Chen, J. Chen, H. Su, C. Li, and J. Zhu, “Contrastive energy prediction for exact energy-guided diffusion sampling in offline reinforcement learning,” in *International Conference on Machine Learning*. PMLR, 2023, pp. 22 825–22 855.

[36] S. Ding, K. Hu, Z. Zhang, K. Ren, W. Zhang, J. Yu, J. Wang, and Y. Shi, “Diffusion-based reinforcement learning via q-weighted variational policy optimization,” *Advances in Neural Information Processing Systems*, vol. 37, pp. 53 945–53 968, 2024.

[37] S. E. Ada, E. Oztop, and E. Ugur, “Diffusion policies for out-of-distribution generalization in offline reinforcement learning,” *IEEE Robotics and Automation Letters*, vol. 9, no. 4, pp. 3116–3123, 2024.

[38] M. Althoff, M. Koschi, and S. Manzinger, “Common-road: Composable benchmarks for motion planning on roads,” in *2017 IEEE Intelligent Vehicles Symposium (IV)*. IEEE, 2017, pp. 719–726.

[39] J. Song, C. Meng, and S. Ermon, “Denoising diffusion implicit models,” *arXiv preprint arXiv:2010.02502*, 2020.

[40] Z. Wang, J. J. Hunt, and M. Zhou, “Diffusion policies as an expressive policy class for offline reinforcement learning,” in *The Eleventh International Conference on Learning Representations*, 2023.

[41] X. Shen, M. Lacayo, N. Guggilla, and F. Borrelli, “Parkpredict+: Multimodal intent and motion prediction for vehicles in parking lots with cnn and transformer,” in *2022 IEEE 25th International Conference on Intelligent Transportation Systems (ITSC)*. IEEE, 2022, pp. 3999–4004.

[42] Y. Li, S. Zhang, M. Jiang, X. Chen, J. Yang, Y. Qian, C. Wang, and M. Yang, “Tactics2d: A highly modular and extensible simulator for driving decision-making,” *IEEE Transactions on Intelligent Vehicles*, vol. 9, no. 5, pp. 4840–4844, 2024.

[43] “Intelligent transport systems - partially-automated parking systems (paps) - performance requirements and test procedures,” ISO 20900:2023, 2023.

[44] J. Reeds and L. Shepp, “Optimal paths for a car that goes both forwards and backwards,” *Pacific journal of mathematics*, vol. 145, no. 2, pp. 367–393, 1990.